Preparation and characterization of polyvinyl alcohol/polyhedral oligosilsesquioxane hybrid membrane for pervaporation separation of high-concentration ε-caprolactam solution

Qin Li[1], Dingding Xiang[2], Yi yin[3], Qian Chen[4], Lei Shi[3] and Wenhai Lin[1,3]*

[1]School of Chemical Engineering, Guizhou Institute of Technology, Guiyang, Guizhou Province, China

[2]School of Chemistry and Chemical Engineering, Qiannan Normal University for Nationalities Duyun, Guizhou Province, China

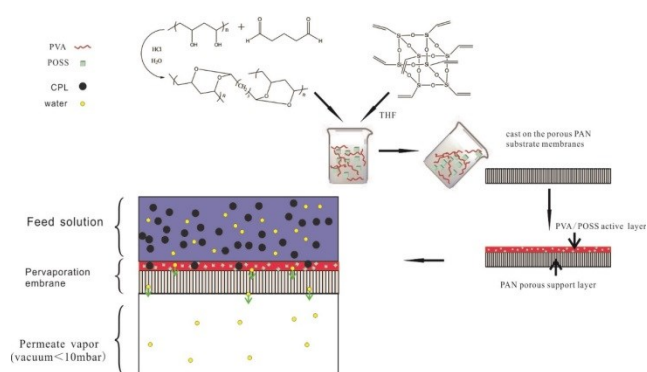[3]Guizhou Zhenhua Qunying Electric Co., Ltd. (State-owned No. 891 Factory) Guiyang, Guizhou Province, China

[4]Guizhou University of Commerce Guiyang, Guizhou Province, China

Received: 26/06/2023, Accepted: 05/10/2023, Available online: 16/10/2023

*to whom all correspondence should be addressed: e-mail: linwenhai@whu.edu.cn

https://doi.org/10.30955/gnj.005210

Graphical abstract

Abstract

We used Vinyl-polyhedral oligosilsesquioxane (POSS) as a modified material and polyvinyl alcohol (PVA) to make a hybrid membrane for the pervaporation membrane separation of high-concentration caprolactam solution. The membranes were characterized by Fourier transform infrared spectroscopy, X-ray diffraction, thermogravimetric analysis, scanning electron microscopy, contact angle measurement, and swelling test. The PVA/POSS hybrid membrane exhibited unique pervaporation performance due to its hydrophobic cage-type nano-silica particles. We evaluated the permeate flux, separation factor, swelling/diffusion selectivity, and activation energy of the hybrid membrane. Evaluation results showed that POSS in the hybrid membrane hindered the crystallization of PVA. The separation flux greatly improved in the separation process of the high-concentration caprolactam solution. The excellent diffusion selectivity brought by POSS also maintained a high separation factor. When the flux reached 2.13 kg m^{-2} h^{-1}, an excellent separation factor of 220 was obtained.

Keywords: Nano-silica particles, permeate flux, separation factor, swelling/diffusion selectivity

1. Introduction

ε-Caprolactam ($C_6H_{11}NO$, CPL) is a versatile industrial organic monomer material that is widely used in the field of plastics and textiles. After being identified by the International Agency for Research on Cancer, it has been considered as the only drug or mixture with no carcinogenicity to humans and experimental animals (IARC Working Group on the Evaluation of Carcinogenic Risks to Humans). Thus, the expansion of CPL applications has been explored. In general, CPL is manufactured by the Beckmann rearrangement conversion of cyclohexanone oxime or the catalytic oxidation of toluene. A large amount of water is produced in the production process, and the water content considerably influences the performance of the final CPL product. The amide bond in CPL is sensitive to heat, and the product deteriorates if the water is removed by ordinary high-temperature distillation. Therefore, high-quality CPL is most commonly produced by three-effect evaporation. However, this traditional process requires high energy and moderate pressure steam and the use of a reaction device that can withstand the corrosiveness of CPL at the process temperature (Yu *et al.*, 2005; van Delden *et al.*, 2006). Especially when the concentration of CPL exceeds 70%, the increase of solute content reduces the partial pressure of water vapor, thus hindering water desalination. Therefore, the temperature of three-effect evaporation must be increased; however, the change increases the energy consumption and causes serious equipment corrosion and scaling problems (Darwish *et al.*, 2006). In the further exploration of the water desalination process involving high-concentration CPL, the reverse osmosis technology encounters extremely strong osmotic pressure brought by the high solute content when it processes the CPL solution with a concentration greater than 70%. Furthermore, the highly concentrated solution aggravates the densification and salt pollution of the reverse osmosis

Li Q., Xiang D.,yin Y., Chen Q., Shi L. and Lin W. (2023), Preparation and characterization of polyvinyl alcohol/polyhedral oligosilsesquioxane hybrid membrane for pervaporation separation of high-concentration ε-caprolactam solution, *Global NEST Journal*, **25**(10), 93-101.

membrane and results in the salt inhibition effect of the concentration gradient across the reverse osmosis membrane, which then becomes impossible to handle. This phenomenon becomes increasingly serious with the increase of CPL concentration (Kaplan *et al.*, 2017). Therefore, methods to separate desalted water from high-concentration CPL solution have been a focus of industrial application research in recent years.

Pervaporation (PV) is a commonly used membrane separation and desalination technology. Its main feature is its ability to desalinate and purify water in a solution under relatively mild conditions; it has the advantages of high separation efficiency, zero pollution, space saving, and low energy consumption (Kalyani *et al.*, 2008). PV technology has unique advantages in the purification of high concentration solutions. The separation principle is based on two differences. One difference is that between the rates of adsorption and diffusion of each component in the liquid mixture through the active layer (pure organic polymer or organic polymer/inorganic hybrid). The other difference is that between the evaporation and separation rates of each component on the membrane surface. Therefore, the inhibitory effect of salt on the separation process is considerably weak. The basic driving force of PV is the difference in the differentiation potentials of all groups in the liquid mixture (Bruggen *et al.*, 2015), which can be carried out at a low operating temperature and reduces the corrosion of salt on equipment. At present, research on PV technology is mainly focused on biochemical, petrochemical, and other chemical-related fields. It has been widely used in the dehydration of high-concentration ethanol and isopropanol (Liao *et al.*, 2017; Liu *et al.*, 2017; Das *et al.*, 2011). With the development of PV technology, the industrial application of water desalting to other liquid mixtures has been recently reported (Kaminski *et al.*, 2018; Liang *et al.*, 2018).

In our previous work, the common hydrophilic nano-silica/PVA hybrid membrane was used for the water desalination of a high-concentration CPL solution by PV (Lin *et al.*, 2012). The PV performance of the membrane is affected not only by the chemical composition but also by the dispersion form of the organic phase/inorganic phase and the interaction of the interface phase. The PV desalination capacity of the hybrid membrane is driven by chemical potential. The principle of vapor permeation can avoid the diffusion of nonvolatile salts into the downstream water vapor to complete desalination and maintain a high separation coefficient (Cao *et al.*, 2018). At present, the PV performance of zeolites with different water/oil wettability and hybrid membranes modified by different organic/inorganic dispersion forms has been studied (Yuan *et al.*, 2004; Teli *et al.*, 2011).

Caged polyhedral oligomericsilsesquioxane (POSS), which has a general structure of $R_nSi_nO_{1.5}$, is a typical nanoparticle. POSS with $n = 8$ is the silica with the smallest diameter and a cage-like nanostructure (Figure 1). Chemical functional groups can be added to the side chain extending around the cage-like structure to provide the special performance required for application scenarios. In recent years, POSS, a type of nano-silica with high consistency, regular structure, and adjustable function, has been widely investigated in the field of organic–inorganic hybrid modification (Zhang *et al.*, 2009; Liu *et al.*, 2007). A series of performance improvements, such as weather resistance, surface hardness, mechanical properties, flame retardant properties, rheological properties, and thermal decomposition properties, can be obtained after adding various POSSs with different functional groups to polymer materials to form hybrid materials (Chen *et al.*, 2010a and 2010b). In recent years, the PV separation of ethanol/water solutions and the removal of sulfur-containing aromatics from long-chain alkane mixtures have been studied using POSS-modified hybrid membranes (Le *et al.*, 2011; Zhang *et al.*, 2011; Konietzny *et al.*, 2014). Existing studies summarized the influence of POSS on the PV separation performance and mechanical properties of modified hybrid membranes and further analyzed the mechanism of the free volume defects caused by the addition of POSS, which results in the change of membrane transport properties (Swapna *et al.*, 2019; Uragami *et al.*, 1998). However, the application of the PV of a POSS-modified hybrid membrane to desalination has not been reported. In the current work, we try to introduce a special cage-like hydrophobic structure for POSS to improve the performance of PV membranes and apply it to high-concentration CPL (70%). On the one hand, the hydrophobicity of the membrane can be increased by using the characteristics of POSS containing hydrophobic groups, which can hinder the separation of CPL on the downstream surface of the membrane. On the other hand, the dispersion of POSS, as a special cage-like nanoparticle, in the polymer chain segment of PVA changes the microstructure of the membrane, increases the diffusion ability of permeable components, and tends to increase the membrane permeability while retaining a high separation factor. We also explore the influence of different operation process factors on the hybrid POSS-modified PV membrane.
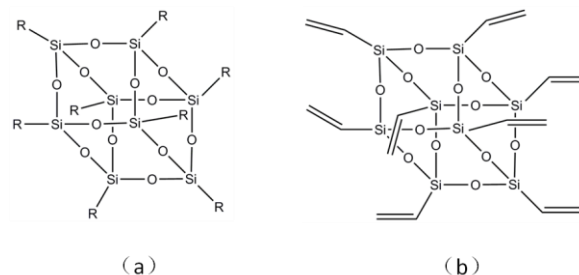
Figure 1. (a) General structure of polyhedral oligomeric silsesquioxane (POSS) and (b) structure of Vinyl-POSS

2. Experimental

2.1. Materials

CPL was purchased from Baling Petrochemical Co., Ltd. PAN (molecular weight cutoff, 5×10^4) porous ultrafiltration membrane was purchased from Hangzhou Water Treatment Technology Development Center. PVA (degree of polymerization 1700±50) and glutaraldehyde (GA, 25% by mass solution) were purchased from

Sinopharm Chemical Reagent Co., Ltd. All other chemical reagents were reagent grade and were used without further purification. Vinyl-POSS (Chen *et al.*, 2010) and deionized water with PV feed solution were made in our laboratory.

2.2. Preparation of hybrid PVA/POSS membranes and PV membranes

2.2.1. Preparation of PVA solution and complex solution

A certain proportion of PVA and deionized water was stirred in a 100 ℃ water bath for 4 h. The mixture was then filtered to obtain 5 wt.% PVA solution. Certain amounts of Vinyl-POSS and tetrahydrofuran were mixed, stirred for 4 h at room temperature, and filtered to obtain 5 wt.% vinyl POSS tetrahydrofuran solution. The Vinyl-POSS tetrahydrofuran solution and PVA solution were mixed in a certain proportion, and the crosslinker GA and hydrochloric acid were added in a certain proportion depending on the amount of PVA. The casting solution for the active layer was obtained by stirring in a conical flask at 25℃ for 24 h. As shown in Table 1, Vinyl-POSS:PVA = 1:9, 3:7, 5:5, which are respectively called M-1, M-2, and M-3 active layer casting solutions. The pure PVA solution without Vinyl-POSS is called the M-0 active layer casting solution.

Table 1. Sample preparation of PVA/POSS hybrids membranes

Membrane	Content (wt.%)	
	Vinyl-POSS	PVA
M-0	0	100
M-1	10	90
M-2	30	70
M-3	50	50

2.2.2. Preparation of pure PVA and PVA/POSS hybrid membranes for PV membrane test

The membrane manufacturing process for testing PV performance was as follows. The PAN porous support membrane was soaked in 5% NaOH solution at 55℃ for 1h, washed with deionized water to neutral, and then immersed in 1N hydrochloric acid solution at room temperature for 20 min. Deionized water was then washed to neutralize the solution. The treated PAN porous support membrane was fixed on a flat and clean glass plate. A certain amount of PVA/POSS casting solution was poured on the surface of the treated PAN porous support membrane and then scraped with a scraper. The glass plate was placed horizontally in a room without dust and air convection. After complete drying at room temperature, the glass plate was placed in a vacuum drying oven at 80℃ for 1h to obtain the hybrid PVA/POSS PV membrane. Pure PVA contrast membrane was prepared via the same process.

2.2.3. Preparation of hybrid PVA/POSS and pure PVA membranes for the active layer test

The active layer for testing other properties was produced as follows. The mixed active layer casting solution was coated on the surface of a clean tetrafluoroethylene plate placed horizontally. The plate was then dried at room temperature in a room without dust and air convection. When the active layer was formed, it was placed in the vacuum drying oven at 80℃ for heat treatment for 1h and then removed for later use.

2.3. Swelling experiments

The equilibrium swelling experiment on the pure PVA active layer and hybrid PVA/POSS active layer in the feed mixture of a concentrated CPL solution (70 wt.%) was carried out at 30℃–50℃. First, the dry active layer mass was accurately weighed as W_D and then immersed in the concentrated CPL solution (70 wt.%) in a sealed container for 48 h to equilibrium. The active layer full of the concentrated CPL solution was removed, and the surface solution was carefully wiped with a filter paper. The weighed mass was W_S. All tests were carried out at least three times, and the results were averaged. Degree of swelling (D_S) was calculated using Equation (1).

$$D_S = \frac{W_S - W_D}{W_D} \times 100\% \tag{1}$$

The calculation of the swelling degree of the CPL in the active layer was carried out as follows. After placing it in an oven at 60 ℃ for 24 h, the CPL was subjected to vacuum treatment for 6 h. The weighed mass was W_A. The swelling selectivity α_S was calculated using Equations (2) and (3).

$$\frac{M_W}{M_C} = \frac{W_S - W_A}{W_A - W_D} \tag{2}$$

$$\alpha_S = \frac{M_W / M_C}{F_W / F_C} \tag{3}$$

M_W and M_C are the mass ratios of water and CPL in the swollen active layer, respectively, and represent the ability of the active layer itself to swell water and CPL. F_W and F_C are the mass values of water and CPL in the feed liquid. The result can explain the interaction of the active layer itself with water and CPL molecules, as well as the interaction between water and CPL molecules.

2.4. Characterization

2.4.1. Fourier transform infrared spectroscopy (FTIR)

After the active layers prepared with the method described in Section 2.2.3 were dried under an infrared lamp. The infrared spectra of the pure PVA and hybrid PVA/POSS active layers were scanned with a Nicolet AVATAR 360 (USA) Fourier transform infrared spectrometer.

2.4.2. X-ray diffraction (XRD)analysis

After being prepared with the method in Section 2.2.3, the active layers were dried under an infrared lamp and then spread flat on a fixture of XRD-6000(Shimadzu, JAP) diffractometer. The XRD measurement conditions were selected for graphite monochromatic CuKα radiation (λ = 1.54 Å) at 40 kV/30 mA. The scanning diffraction angle ranged from 5° to 60°, and the scan rate was set to 4°/min to identify differences in the crystal structures in the active layers.

2.4.3. Thermogravimetric (TG)analysis

The active layer prepared following the method in Section 2.2.3 was cut into approximately 5–10 mg and placed in an Al_2O_3 crucible. Scanning was carried out at a heating rate of 10℃/min at a N_2 flow rate of 50 ml/min by using a SETSYS 16 (France) instrument at a temperature ranging from 20℃to 600℃.

2.4.4. Scanning electron microscopy (SEM)

The hybrid PV membrane prepared according to the method in Section 2.2.2 was finely chopped under liquid nitrogen cooling and then sputtered with a thin layer of gold on the surface. The surface/section morphology of the pure PVA and hybrid PVA/POSS membranes was examined by using a FEI Quanta 200 (Holland) scanning electron microscope.

2.4.5. Contact angle experiment

Contact angle was measured using a DSA100 instrument (Kruss Company, Germany) with a drop angle observation system. The relative hydrophilicity of the surface of the pure PVA membrane and that of the surface of the hybrid PVA/POSS membrane were determined by measuring the static contact angle of 5 µl of H_2O on the surface of each membrane with a static sessile drop method. The membrane to be tested was vacuum dried before the test. The measurement time was set to less than 10 s to reduce the influence of water evaporation. Contact angle θ was calculated using Equation (4) (Uragami *et al.*, 1998):

$$\theta = cos^{-1} \frac{cos\theta_a + cos\theta_r}{2} \quad (4)$$

Where θ_a is the advancing contact angle and θ_r is the receding contact angle. The final contact angle is the average calculated result after repeating all experiments at least three times.

2.4.6. PV experiments

The tested membrane (effective area of 34.32cm^2) was soaked and equilibrated for approximately 1–2 h in the feed mixture with concentrated CPL (70 wt.%). After the system was stable, the PV test was initiated. The steam permeating from the downstream side in a cold well immersed in a liquid nitrogen tank (internal air pressure of 1 mm Hg) was collected. The collection time interval was then fixed.

The PV experiment was carried out in the temperature range of 30℃–50℃. The composition of the liquid feed was analyzed by measuring the refractive index at the same temperature. An appropriate supplement was made to keep the composition constant. After collection in cold well, the sample was sealed. When the temperature was returned to room temperature, the sample was weighed, and the result served as basis for the calculation of the permeability flux. The content of CPL in the cold well was determined by gas chromatography (GC) (Zhang *et al.*, 2007). The gas chromatograph sp3400 (China) was equipped with an FID detector and a 2 m×6 mm PEG-20M capillary column. The test column temperature was 170℃, and nitrogen was used as a carrier gas at a flow rate of 30 mL/min. The results of all PV experiments were the average of the four repeated experiments with a mean standard deviation of less than 10%.

Equations (5) and (6) were respectively used to calculate J (permeation flux) and α (separation factor) for the evaluation of the separation performance of the pure PVA and PVA/POSS membranes:

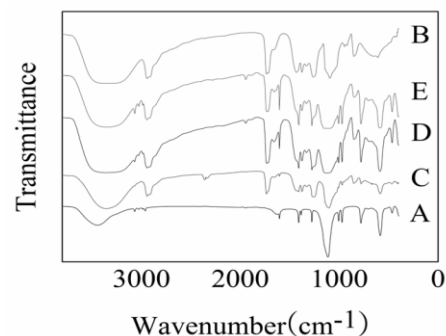$$\alpha = \frac{y_w / y_{CPL}}{x_w / x_{CPL}} \quad (5)$$

$$J = \frac{W}{At} \quad (6)$$

where W (g) is the weight of the permeate in the cold well, A(m^2) is the active membrane area, t (h) is the operation time, y_w/y_{CPL} is the mole fraction ratio of water and CPL in the permeate, and x_w/x_{CPL} is the mole fraction ratio of water and CPL in the feed.

3. Results and discussion

### 3.1. Membrane characterization

3.1.1. FTIR analysis

Figure 2. FTIR spectra of pure PVA active layer M-0 (e), pure Vinyl-POSS(a) and PVA/POSS hybrid active layers M-1(c), M-2(d),M-3(e)

The infrared spectra of pure PVA, pure vinyl POSS, and hybrid PVA/POSS active layer are shown in Figure 2. The infrared spectrum of pure PVA is illustrated in Figure 2B. The broad peak near 3300 cm^{-1} is the stretching vibration peak of the OH group. The small peak near 2940 cm^{-1} is the symmetric stretching vibration peak and the anti-symmetric stretching vibration peak of the C–H bond. The stretching vibration peak of the C=O group without hydrolysis in PVA is near 1720 cm^{-1}. The peak band near 1200-1480cm^{-1} is the deformation vibration peak of CH_2.The peak band from 1094cm^{-1} to 1200 cm^{-1} is the vibration peak of the C–O and C–O–C groups produced by the GA crosslinking reaction and proves the crosslinking of PVA (Zhang *et al.*, 2007). The infrared spectrum of pure vinyl POSS is shown in Figure 2A. The peak at 1110 cm^{-1} is the stretching vibration peak of Si–O–Si, and the stretching vibration peak at 780 cm^{-1} is the stretching vibration peak of Si–C. At 1605 cm^{-1} is the stretching vibration peak of vinyl C=C in vinyl POSS. At 1410, 970, 1275, and 1000 cm^{-1} are the bending vibration peaks of the in-plane and out-of-plane C–H. At 475 and 812 cm^{-1} are the skeleton vibration peaks of Si–O–Si, which fully prove that the structure of vinyl POSS simultaneously

contains unsaturated double bond and organosilicon skeleton (Chen *et al.*, 2010). Figures 2C-E show the infrared spectra of the hybrid PVA/POSS active layers (M-1, M-2, M-3). The typical vibration peak of the Si–O–Si framework is at 475cm⁻¹(Lin *et al.*, 2012). With the increase in the proportion of POSS in the hybrid active layers, the peak type becomes evident, whereas no FTIR peak is observed in pure PVA (M-0). The results show the different proportions of POSS and PVA in the hybrid active layer. The peak at 1605 cm⁻¹remains evident and thus proves that the C=C bond still exists in the process of forming the active layer and that the hybrid active layers could be further subjected to chemical reaction modification. The infrared spectrum shows that POSS is coated in PVA to form the hybrid PVA/POSS active layers.

3.1.2. XRD analysis
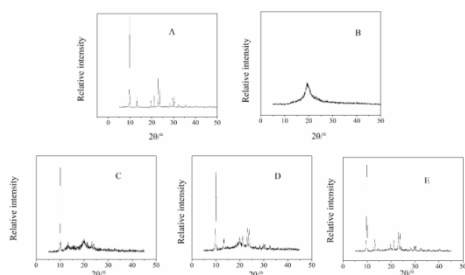
Figure 3. XRD patterns of pure Vinyl-POSS(A), pure PVA active layer M-0 (B)and PVA/POSS hybrid active layers M-1(C), M-2(D),M-3(E)

The XRD patterns of pure vinyl POSS, pure PVA, and hybrid PVA/POSS active layers are shown in Figure 3. Figure 3A presents the XRD pattern of pure vinyl POSS, showing a sharp peak at 2θ=9.8° and other peaks at 13.0°, 19.5°, 21.0°, 22.8°, 23.6°, and 29.6°; this result proves that vinyl POSS is a highly crystalline compound (Chen *et al.*, 2010). A peak occurs between 15° and 30° for the pure PVA active layer, and the center of peak is approximately 20° (Figure 3B), which is a typical high crystalline polymer spectrum. When PVA and POSS form a hybrid active layer, the peak at approximately 20° becomes increasingly low and gentle, and the characteristic peaks of POSS remain evident with the increase in the amount of POSS. The results show that the crystallization process of PVA is affected by POSS and that the crystallinity of the hybrid PVA/POSS active layers decreases with the increase of POSS. Additional channels form in the active layer for water molecules to pass through in the PV process. Each characteristic peak of POSS is completely preserved. This result indicates that after the formation of the hybrid active layer, POSS still maintains its own cage structure well. This characteristic influences the results of PV.

3.1.3. TG analysis

The thermal stability order of the active layers is M-3>M-2>M-1. Thermal decomposition process of the active layer is hindered gradually, and its heat resistance is improved as the POSS content increases. As a stable cage silica particle, POSS is generally believed to hinder the thermal movement of the polymer chain segment of PVA when dispersed in PVA and delay the thermal decomposition

process during the thermal decomposition of the hybrid active layer. The thermal decomposition of silica itself requires additional energy to destroy the cage structure. Another reason is that when POSS particles are dispersed in PVA, the network structure formed in the thermal decomposition process prevents the outward diffusion of thermal decomposition products, such as volatile gases; this condition further hinders the thermal decomposition reaction (Chen *et al.*, 2010) Figure 4.
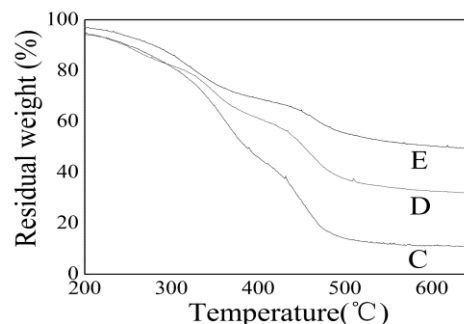
Figure 4. TGA results of PVA/POSS hybrid active layers M-1(C), M-2(D), M-3(E)

3.1.4. SEM analysis

As shown in Figures 5A-C and 5D-F, with the increase of POSS content, the surface of the PV membrane becomes rough, and the crystal structure of POSS becomes increasingly evident. The rough surface structure is conducive to water leaving from the membrane surface. POSS in the membrane causes a large number of pores for the permeable components to pass through, and this condition exerts a positive effect on the increase of PV flux. When the content of POSS is low (30 wt.%), the combination of POSS and PVA is close, and the membrane surface is relatively compact and continuous. When the content of POSS increases to 50 wt.%, PVA and POSS have a certain degree of phase separation. We previously studied the cross section and surface of pure PVA with SEM and found that the surface of the membrane is dense and smooth and that no holes and phase separation interface form on the cross section of the membrane (Lin *et al.*, 2012). The difference between the surface and the internal structure of the hybrid PVA/POSS membrane and the PVA hybrid membrane determines their differences in PV performance.
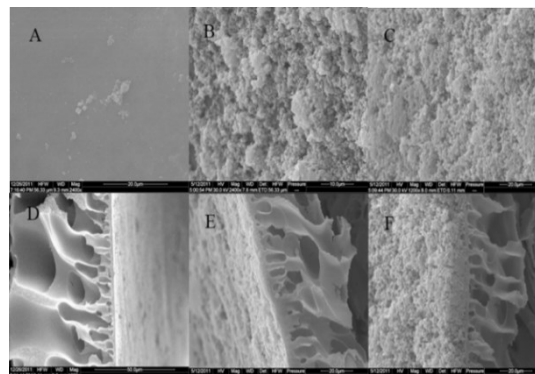
Figure 5. External surface and cross-section morphologies of PVA/POSS hybrid membranes M-1(A, D) M-2(B,E) and M-3(C,F)

3.1.5. Contact angle analysis

Table 2. Contact angles of water on pure PVA and PVA/POSS hybrid membranes

| Abbreviations	proportion in the membrane (wt.%)		Contact angle (°)
	PVA	Vinyl-POSS	
M-0	100		78±1
M-1	90		12±1
M-2	70		13±1
M-3	50		11±1

The contact angle test results of the pure PVA and hybrid PVA/POSS membranes are shown in Table 2. The data show that the addition of POSS reduces the contact angle of the membrane surface and that the contact angles of all hybrid membranes are much lower than that of pure PVA. Hence, water molecules easily dissolve into the surface of the hybrid membrane. From the SEM and XRD patterns, we find that when PVA and POSS are mixed together, the POSS wrapped in the PVA membrane seriously interferes with the crystallization of PVA. Unlike the pure PVA with a smooth and dense surface, the hybrid membrane becomes rough, and the amorphization of the membrane surface causes a decrease in the contact angle. This result proves that with the addition of POSS, the hybrid membrane is more favorable than the pure PVA membrane in terms of the entry of water molecules in the liquid phase during PV.
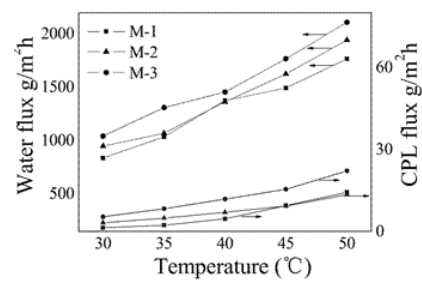
3.2. PV characteristics

3.2.1. Test of PV of hybrid PVA/POSS membrane
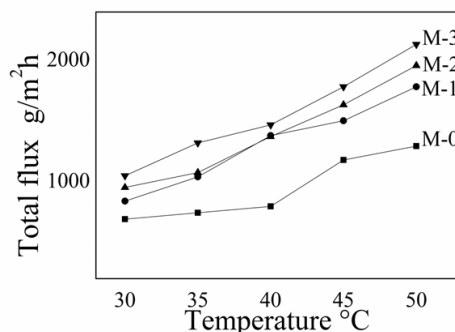
Figure 6. Flux of PV for 70 wt. % aqueous CPL solution in pure PVA membrane and PVA/POSS hybrid membranes at different temperatures
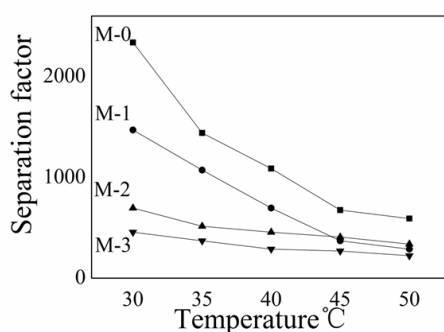
Figure 7. Separation factor of PV for 70 wt. % aqueous CPL solution in pure PVA membrane and PVA/POSS hybrid membranes at different temperatures


Figure 8. Flux of CPL and water of PV for 70 wt. % aqueous CPL solution in pure PVA membrane and PVA/POSS hybrid membranes at different temperatures

Figures 6-7 show that the permeation flux of the hybrid PVA/POSS membrane is greatly improved relative to that of the pure PVA membrane. The separation factor is also decreased. As a nano-silica particle, POSS enters the segment of PVA to form a gap between two phases. These voids facilitate the transfer of water molecules in the membrane and reduce the penetration resistance of water molecules. Another reason for the increase of the permeation flux is that the addition of POSS reduces the crystallinity of PVA (Figure 3). In addition, when a large amount of hydrophobic POSS particles are present on the surface of the active layer, the water molecules easily leave the surface of the active layer, resulting in the increase in the penetration flux. As POSS content increases, the separation factor decreases (Figure 7) possibly because POSS increases the hydrophobicity of the membrane and easily swells the CPL into the membrane. However, Figure 8 illustrates that most of the permeation is water, with CPL only accounting for a small proportion. Hence, the hybrid PVA/POSS membrane is suitable for CPL dehydration.

Figures 6-8 illustrate that when the temperature increases, the water flux and CPL flux increase because the polymer segment movement accelerates as the temperature rises and the internal free volume increases (Fujita *et al.*, 1960). Furthermore, the separation factor decreases with increasing temperature because the increase in temperature accelerates the movement of CPL molecules (Kulkarni *et al.*, 2006). Therefore, as the temperature rises, the corresponding separation factor decreases (Figure 7).

3.2.2. Analysis of swelling degree and swelling/diffusion selectivity of hybrid PVA/POSS active layers
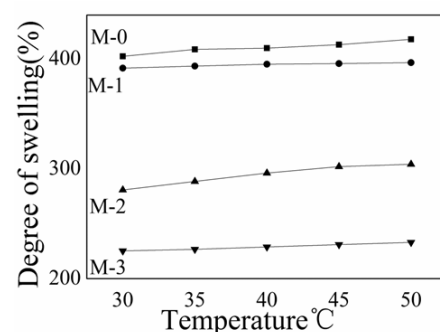
Figure 9. The degree of swelling in 70 wt. % CPL aqueous solution of pure PVA and PVA/POSS hybrid active layers at different temperatures
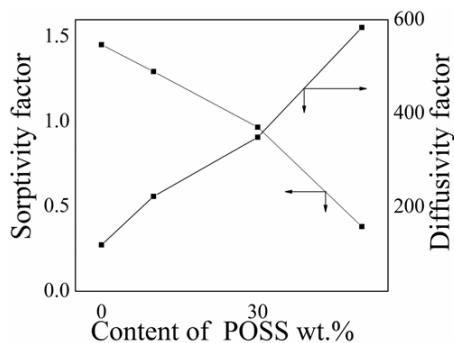
Figure 10. Sorptivity/diffusivity selectivity results of pure PVA and PVA/POSS hybrid active layers at 50 ℃

Vinyl-POSS is hydrophobic and has a regular cage structure. When PVA in the hybrid active layer is swollen by water, POSS maintains its stable structure and morphology. This property causes the varied swelling conditions of the hybrid PVA/POSS active layers relative to the ordinary hydrophilic silica sol/PVA active layer. Figure 9 shows that the swelling degree of the hybrid PVA/POSS active layer increases slowly with the increase of temperature. However, with the increase of the POSS amount, the swelling degree of the hybrid active layer decreases greatly. This result is due to POSS hindering the extension of the PVA chain among the molecular segments of PVA, thus limiting the free volume inside the hybrid active layer. POSS is a highly crystalline hydrophobic nano-silica particle with minimal water swelling ability. When the content of POSS increases, the swelling degree of the active layer decreases. Swelling experiments show that the addition of POSS can control the excessive swelling of PVA in the hybrid active layer.

Diffusion selectivity α_D is calculated using Equation (7):

$$\alpha_D = \frac{\alpha}{\alpha_S} \tag{7}$$

where α is the separation factor and α_S is the sorptivity factor(Kaminski *et al.*, 2018).

The effects of POSS content on the swelling selectivity and diffusion selectivity of the hybrid active layer are shown in Figure 10. Contrary to that of nano-silica sol with hydrophilic groups on the surface, the diffusion selectivity of the hybrid active layer increases significantly when the POSS content increases. This result is attributed to the ability of water to desorb in the active layer to increase with the addition of POSS. Given the increase of the POSS content, the interfacial interaction between the organic–inorganic phase is enhanced, and a relatively loose structure is formed. On the surface of the POSS particles is a hydrophobic vinyl group, and its binding ability to water is lower than that of PVA. Thus, the active layer body can easily leave the surface of the active layer with a high POSS content. Moreover, the water molecules pass through the active layer and leave the active layer surface quickly. As a result, the diffusion selectivity increases. The swelling selectivity of the hybrid PVA/POSS active layer gradually decreases as the POSS content increases. This result may be due to POSS itself being a hydrophobic structure, which is more difficult to combine with water than PVA in the process of swelling. By comparing the

diffusion selectivity and swelling selectivity, we find that the swelling selectivity factor α_S of the hybrid PVA/POSS active layer is significantly smaller than the diffusion selectivity factor α_D. This result shows that the POSS-PVA phase forms a hybrid active layer. The hybrid active layers have a slightly lower swelling selectivity for CPL and water than pure PVA. However, the diffusion selectivity is greatly improved due to changes in surface properties. The selective separation ability of the hybrid PVA/POSS active layers is heavily dependent on diffusion selectivity, that is, the difference in the speed at which the CPL and water molecules leave the active layer surface to enter the downstream. Moreover, the selection ability at the diffusion step exerts a great influence on the PV.

3.2.3. Analysis of activation energy of hybrid PVA/POSS membranes
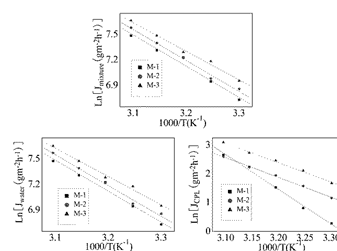
Figure 11. Activation energy analysis of total PV flux, water PV flux, and CPL PV flux

Table 3. Evaluated activation energy data for the PVA/POSS hybrid PV membranes

ΔE_a Membrane	Activation energy(kJ/mol)		
	E_m	E_w	E_{CPL}
M-1	30.60	30.32	100.71
M-2	30.24	30.11	57.46
M-3	27.99	27.78	56.33

Figure 11 clearly illustrates that the total flux, water flux, and CPL flux are in good agreement with the Arrhenius equation with temperature changes. For the hybrid PVA/POSS membranes, the way in which components permeate through PV is still constrained by the Arrhenius equation, and temperature is a decisive operational factor.

Table3 shows the flux activation energy calculated by (ln (E_J) vs. 1/T). The permeation flux activation energy (E_m) values of the M-1, M-2, and M-3 membranes are 30.60, 30.24, and 27.99 kJ/mol, respectively. This result indicates that the permeate component needs to cross an energy barrier through the membrane. As the temperature of the feed increases, the membrane becomes increasingly susceptible to penetration by the permeate. The hybrid PVA/POSS membrane has an organic–inorganic hybrid structure different from that of the pure PVA membrane. The POSS in the membrane is different from the hydrophilic silica sol because its surface is hydrophobic. Therefore, the interaction with water does not change much when the temperature rises, and the E_w change is not evident. By contrast, the changes in E_{CPL} are significant. The CPL's split activation energy (E_{CPL}) is higher than the water flux activation energy (E_w) during the same

PV process of all membranes. This result indicates that the energy barrier that CPL molecules need to overcome downstream through the membrane is much larger than that of water molecules. Combined with the analysis of Figure 10, the results show that the hybrid PVA/POSS membrane has a low binding force to water due to the increased hydrophobicity of the surface. This condition causes the water component to diffuse easily into the downstream gas phase, as opposed to the CPL, which imparts the membrane with a high selectivity for water. The special organic–inorganic hybrid structure of the hybrid PVA/POSS membrane is suitable for PV separation of CPL/water systems. From the separation mechanism, POSS causes the hydrophobicity of the membrane surface to be different from that of the hybrid PVA/hydrophilic SiO_2 membrane. Increased flux is obtained while maintaining a good separation factor.

Table 4. Comparison with the literature

Membrane	Content of CPL in feed solution (wt. %)	T (K)	Flux(gm^{-2}h^{-1})	Separation factor	Reference
PVA	30	328	900	1500	27
PVA-CS	30	323	600	1800	31
Nano silica/PVA	30	323	2911	76	13
NaAlg-PVP	30	323	820	2450	32
PVA /POSS M-2	30	323	1958	337	This Work
PVA /POSS M-3	30	323	2133	222	This Work

4.   Conclusion

Vinyl-POSS and PVA were synthesized into an organic–inorganic active hybrid layer, and a novel PV membrane using PAN as a support layer was prepared for the separation of a high-concentration CPL solution. The FTIR, XRD, and SEM spectra demonstrated that the interaction between POSS and PVA affected the crystallization of PVA. The highly crystalline structure of the cage-like POSS was still retained. Through the PV experiments on high-concentration CPL/water systems, we evaluated the PV performance of the hybrid PVA/POSS active layers. With the increase of POSS content in the hybrid active layer, the permeation flux tended to increase gradually. However, the separation factor decreased but could still maintain a high level (>220). The analysis of the swelling selectivity and diffusion selectivity in the combined swelling test revealed that during the separation process, the diffusion selectivity of the osmotic component leaving the active layer surface into the downstream gas phase was critical to the selectivity of the membrane. The hydrophobic structure of the POSS surface affected the PV process. The analysis of the activation energy supported this conclusion. CPL could not easily enter the gas phase under the hydrophobic surface. However, the hydrophobic POSS accelerated the transfer of CPL inside the membrane. The influence on water was reversed, and the overall effect was complex. The permeation flux of the hybrid PVA/POSS membrane in the PV separation of the 70 wt.% the CPL/water system reached 2.13 kg/m^{2}h, which was slightly lower than that of the hybrid PVA/SiO$_2$ membrane (Table 4). Nevertheless, a high separation factor was obtained, and such result is favorable for the industrial PV application of high-concentration CPL/water systems. The results also indicate that regular nano-silica particles (such as POSS) with specific functional groups and specific structures can be introduced into the field of PV to produce hybrid active layers and thereby expand membrane manufacturing methods in the field of PV.

References

Bruggen V. and Patricia B.L. (2015). Pervaporation, Progress in filtration and separation, **4**, 101–154, https://doi.org /10.1016/B978-0-12-384746-1.00004-5.

Cao Z., Zeng S. and Xu Z. (2018). Ultrathin ZSM-5 zeolite nano sheet laminated membrane for high-flux desalination of concentrated brines, *Science advances*, **4(11)**, eaau8634. https://doi.org/10.1126/sciadv.aau8634.

Chen D., Nie J. and Yi S. (2010b). Thermal behaviour and mechanical properties of novel RTV silicone rubbers using divinyl-hexa[(trimethoxysilyl)ethyl]-POSS as cross-linker, *Polymer Degradation and Stability*, **95(4)**, 618–626, https://doi.org/10.1016/j.polymdegradstab.2009.12.002.

Chen D., Yi S. and Wu W. (2010a). Synthesis and characterization of novel room temperature vulcanized (RTV) silicone rubbers using Vinyl-POSS derivatives as cross linking agents, *Polymer,* **51(17)**, 3867–3878, https://doi.org/10.1016/j.polymer.2010.06.028.

Cussler E.L. (1990). Membranes containing selective flakes, *Journal of Membrane Science*, **52(3)**, 0–288, https://doi.org/ 10.1016/s0376-7388 (00)85132-7.

Darwish M.A., Al-Juwayhel F. and Abdulraheim H.K. (2006). Multi-effect boiling systems from an energy viewpoint, *Desalination,* **194(1–3)**, 22–39, https://doi.org/10.1016/ j.desal.2005.08.029.

Das P., Ray S.K. and Kuila S.B. (2011). Systematic choice of crosslinker and filler for pervaporation membrane: A case study with dehydration of isopropyl alcohol–water mixtures by polyvinyl alcohol membranes, *Separation and Purification Technology*, **81(2)**, 159–173, https://doi.org/10.1016/ j.seppur.2011.07.020.

Fujita H., Kishimoto A. and Matsumoto.K. (1960). Concentration and Temperature Dependence of Diffusion Coefficients for Systems Polymethyl Acrylate and n-Alkyl Acetates, *Transactions of the Faraday Society*, **56,** https://doi.org/10.1039/tf9605600424

IARC Working Group on the Evaluation of Carcinogenic Risks to Humans. (2012). Chemical agents and related occupations, Iarc monographs on the evaluation of carcinogenic risks to humans, 100(PT F), 9–562.

Kalyani S., Smitha B. and Sridhar S. (2008). Pervaporation separation of ethanol-water mixtures through sodium alginate membranes, *Desalination*, **229(1–3)**, 68–81, https://doi.org/10.1016/j.desal.2007.07.027

Kaminski W., Marszalek J. and Tomczak E. (2018). Water desalination by pervaporation-Comparison of energy consumption, Desalination, **433,** 89–93, https://doi.org/10.1016/j.desal.2018.01.014.

Kaplan R., Mamrosh D. and Salih H.H. (2017). Assessment of desalination technologies for treatment of a highly saline brine from a potential CO_2 storage site, *Desalination*, **404**, 87–101, https://doi.org/10.1016/j.desal.2016.11.018.

Konietzny R., Koschine T. and Tzke K. (2014). POSS-hybrid membranes for the removal of sulfur aromatics by pervaporation, *Separation and Purification Technology*, **123**, 175–182, https://doi.org/10.1016/j.seppur.2013.12.024.

Kulkarni S.S., Tambe S.S. and Kittur A.A. (2006). Modification of tetraethylorthosilicate crosslinked poly (vinyl alcohol) membrane using chitosan and its application to the pervaporation separation of water–isopropanol mixtures, *Journal of Applied Polymer Science*, **99(4)**, 1380–1389, https://doi.org/10.1002/app.22514.

Le N.L., Wang Y. and Chung T.S. (2011). Pebax/POSS mixed matrix membranes for ethanol recovery from aqueous solutions via pervaporation, *Journal of Membrane Science*, **379 (1–2)**, 174–183, https://doi.org/10.1016/j.memsci.2011.05.060.

Li Q., Yu P. and Zhu T. (2010). Pervaporation performance of crosslinked PVA and chitosan membranes for dehydration of caprolactam solution, *Desalination and Water Treatment,* **16(1–3)**, 304–312, https://doi.org/10.5004/dwt.2010.1568.

Liang B., Li Q. and Ca B. (2018). Water permeance, permeability and desalination properties of the sulfonic acid functionalized composite pervaporation membranes, *Desalination,* **433**, 132–140, https://doi.org/10.1016/j.desal.2018.01.028.

Liao Y.L., Hu C.C. and Lai J.Y. (2017). Crosslinked polybenzoxazine based membrane exhibiting in-situ self-promoted separation performance for pervaporation dehydration on isopropanol aqueous solutions, *Journal of Membrane Science*, **531**, 10–15, https://doi.org/10.1016/j.memsci.2017.02.039.

Lin W.H., Zhu T.R., Li Q., Yi S.P. and Li Y. (2012). Study of pervaporation for dehydration of caprolactam through PVA/nano silica composite membranes, *Desalination*, **285,** 39–45, https://doi.org/10.1016/j.desal.2011.09.028

Liu J. and Bernstein R. (2017). High-flux thin-film composite polyelectrolyte hydrogel membranes for ethanol dehydration by pervaporation, *Journal of Membrane Science*, **534**, 83–91, https://doi.org/10.1016/j.memsci.2017.04.018.

Liu Y., Zeng K. and Zheng.S. (2007). Organic–inorganic hybrid nano composites involving novolac resin and polyhedral oligomeric silsesquioxane, *Reactive and Functional Polymers*, **67(7)**, 627–635. https://doi.org/10.1016/j.reactfunctpolym.2007.04.002.

Swapna V.P., Nambissan P.M.G. and Selvin T.P. (2019). Free Volume Defect and Transport Properties of Mechanically Stable Polyhedral Oligomeric Silsesquioxane Embedded Poly (vinyl alcohol)-Poly(ethylene oxide) Blend Membranes, *Polymer international*, **68,** 1280–1291, https://doi.org/10.1002/pi.5815

Swapna V.P., Thomas S.P. and Jose T. (2019). Mechanical properties and pervaporation separation performance of CTAB-modified cage-structured POSS-incorporated PVA membrane, *Journal of materials science*, https://doi.org/10.1007/s10853-019-03479-8

Teli S.B., Calle M. and Li N. (2011). Poly (vinyl alcohol)-H-ZSM-5 zeolite mixed matrix membranes for pervaporation separation of methanol–benzene mixture, *Journal of Membrane Science*, **371(1–2)**, 171–178, https://doi.org/10.1016/j.memsci.2011.01.033.

Uragami T., Tsukamoto K. and Inui K. (1998). Pervaporation characteristics of a benzoyl chitosan membrane for benzene-cyclohexane mixtures, *Macromolecular Chemistry and Physics*, **199(1)**, 49–54, https://doi.org/10.1002/(SICI)1521-3935(19980101)199:13.3.CO;2-2.

van Delden M.L., Kuipers N.J.M. and de Haan A.B. (2006). Selection and evaluation of alternative solvents for caprolactam extraction, *Separation and Purification Technology*, **51,** 219–231, https://doi.org/10.1016/j.seppur.2006.02.003.

Yu P., Zhu Z.H., Luo Y.B., Hu Y.H. and Lu S.J. (2005). Purification of caprolactam by means of an electrode ionization technique, *Desalination,* **174**, 231–235, https://doi.org/10.1016/j.desal.2004.09.013.

Yuan W., Lin Y.S. and Yang W. (2004). Molecular Sieving MFI-Type Zeolite Membranes for Pervaporation Separation of Xylene Isomers, *Journal of the American Chemical Society*, **126(15)**, 4776–4777, https://doi.org/10.1021/ja031653t.

Zhang L., Yu P. and Luo Y.B. (2007). Dehydration of caprolactam-water mixtures through cross-linked PVA composite pervaporation membranes, *Journal of Membrane Science*, **306**, 93–102, https://doi.org/10.1016/j.memsci.2007.08.036

Zhang Q.G., Fan B.C. and Liu Q.L. (2011). A novel poly (dimethyl siloxane)/poly (oligosilsesquioxanes) composite membrane for pervaporation desulfurization, *Journal of Membrane Science*, **366(1–2)**, 335–341, https://doi.org/10.1016/j.memsci.2010.10.022.

Zhang W., Zhuang X., Li X., Lin Y., Bai J. and Chen Y. (2009). Preparation and characterization of organic/inorganic hybrid polymers containing polyhedral oligomeric silsesquioxane via RAFT polymerization, *Reactive and Functional Polymers*, 69(2), 124–129. https://doi.org/10.1016/j.reactfunctpolym.2008.11.009.

Zhu T., Luo Y. and Lin Y. (2010). Study of pervaporation for dehydration of caprolactam through blend NaAlg–poly (vinyl pyrrolidone) membranes on PAN supports, *Separation and Purification Technology*, **74(2)**, 242–252. https://doi.org/10.1016/j.seppur.2010.06.012.